



System Optimization for a 2-Stroke Diesel Engine with a Turbo Super Configuration Supporting Fuel Economy Improvement of Next Generation Engines

2014-32-0011

20149011

Published 11/11/2014

Pavel Brynych and Jan Macek

Czech Technical Univ.

Pascal Tribotte

Renault

Gaetano De Paola and Cyprien Ternel

IFP Energies Nouvelles

CITATION: Brynych, P., Macek, J., Tribotte, P., De Paola, G. et al., "System Optimization for a 2-Stroke Diesel Engine with a Turbo Super Configuration Supporting Fuel Economy Improvement of Next Generation Engines," SAE Technical Paper 2014-32-0011, 2014, doi:10.4271/2014-32-0011.

Copyright © 2014 SAE International and Copyright © 2014 SAE Japan

Abstract

The objective of this paper is to present the results of the GT Power calibration with engine test results of the air loop system technology down selection described in the SAE Paper No. 2012-01-0831. Two specific boosting systems were identified as the preferred path forward: (1) Super-turbo with two speed Roots type supercharger, (2) Super-turbo with centrifugal mechanical compressor and CVT transmission both downstream a Fixed Geometry Turbine. The initial performance validation of the boosting hardware in the gas stand and the calibration of the GT Power model developed is described. The calibration leverages data coming from the tests on a 2 cylinder 2-stroke 0.73L diesel engine. The initial flow bench results suggested the need for a revision of the turbo matching due to the big gap in performance between predicted maps and real data. This activity was performed using Honeywell turbocharger solutions spacing from fixed geometry waste gate to variable nozzle turbo (VNT). New simulations results recommend VNT as it offers a higher potential to reduce BSFC with increase power and low end torque output than the original matching. For the high pressure stage the mechanical Roots type and the CVT superchargers have been assessed and the latter one has been identified having higher power adsorption than traditional positive displacement supercharger. This has allowed the supplier to work on an optimization of the units. Ultimately the VNT with CVT supercharger has been assessed on engine and it allowed confirming the validity and accuracy of the GT Power model after its calibration.

Introduction

The framework of this scientific research falls within the need to assess alternative combustion systems to the four-stroke single turbo Diesel engine with the intent to sustain the need to reduce below 95g/km the carbon emission by 2020. Two-stroke engines promise natural internal gas recirculation supporting PCCI-like, low-temperature combustion with limited emissions of soot and nitrogen oxides. In this context the activity has revealed the air system as a key element to enable achieving ultra low emission levels with an ultra downsized two-stroke diesel engine for mini and sub-mini vehicle segments.

Low exhaust gas temperature of two-stroke diesel and the need for both high scavenging ratio (i.e., large positive difference between boost pressure and turbine inlet pressure) and high boost pressure excluded the use of a single turbocharger only. High boost pressure was needed due to limited quality of cross-scavenging with reversed tumble for applied 2+2 valve cylinder head. Instead of a single turbocharger layout, the combinations of a supercharger - turbocharger group or electrically assisted turbocharger have to be used. The requirements on high turbocharger efficiency, which can reduce the power input to a supercharger, are clear. Since the torque of engine should ensure good drivability over a wide range of engine speed, boost pressure control is necessary. On the other hand, any turbocharger control reduces the resulting overall efficiency of the whole charging group. The turbine waste gate reduces the overall efficiency more than the variable nozzle turbine. Nonetheless, the turbine waste gate is used in narrower operation range than the variable nozzle turbine. Unlike in the case four-stroke engine, the driving power of a supercharger cannot be recuperated

back to engine crankshaft, since there is no pumping loop in the indicator diagram and all pressure difference between inlet and exhaust manifold is devoted to overcoming pressure losses in the pipe system.

Due to those reasons, the careful optimization of the air loop has to be done for real conditions at an engine, including (1) all pressure losses (all pipe splits or joints, inlet filter, intercoolers, EGR pipe splits or venturies - if used, DPF upstream or downstream a turbine, exhaust muffler, etc.) and (2) unsteadiness, i.e. pressure waves influencing both gas exchange and turbine/compressor performance. Unlike in the four-stroke engine case, operation conditions of all components are closely interconnected. Scavenging, e.g., needed for reasonable fresh gas purity in a cylinder, dilutes burnt gas transferred to a turbine and reduces significantly its temperature, i.e., enthalpy usable at a turbine. Simulation may be used for an early stage of design, if appropriately calibrated by experimental data, of all pressure boosting devices together with intercoolers, aftertreatment equipment and pipe elements, supported by 3-D CFD modelling.

The workflow of the whole air-loop optimization has consisted in

- experimental, steady-flow tests of all potentially useable turbochargers, superchargers and intercoolers
- prediction of pressure losses of other devices in air-loop using CFD steady flow simulations
- building and calibrating 1-D (GT Power) model of the whole system (combustion model was based on single cylinder research engine tests)
- optimization of different air-loop system lay-outs by GT Power and the selection of the best solution
- designing and manufacturing the selected system
- Tests of the engine, validation of results and feedback to the simulation tools used for detailed optimization.

The current paper describes the main results achieved during system optimization and the features of VNT turbocharger compared to a WG high-efficiency turbine.

Summary of Previous Work

Main Issues of Two-Stroke Engine Pressure Charging

Scavenging of two stroke engine requires the positive pressure difference between inlet and exhaust systems. The excess of scavenging air dilutes burnt gas and decreases exhaust temperature. The inlet-exhaust pressure difference has to ensure the necessary flow-rate during scavenging, depending significantly on available flow area of engine valves during scavenging period.

The fast assessment of the system may be done using algebraic model of steady flow through engine with overlapped valve opening, turbocharger turbine-compressor power balance and exhaust gas temperature calculated from energy balance of a reciprocating two-stroke engine. All parameters

describing gas exchange quality have to be estimated from experience or found by more deep 1-D or 3-D simulations combined with specific scavenging experiments.

The SAE definition of gas exchange parameters - [1] has been used, namely delivery ratio λ_d (inlet port mass flow rate \dot{m}_{im} / perfect-scavenging trapped mass flow rate based on engine displacement volume V_s , speed n_E and density in inlet manifold at pressure p_{im} and temperature T_{im}), charging ratio λ_{ch} (trapped mass/perfect-scavenging trapped mass) and scavenging efficiency η_{scav} (fresh charge mass reduced to overall oxygen contents including rest gas/trapped mass). Moreover, turbocharger and supercharger efficiencies (both isentropic + mechanical) η_{TC} , η_{SC} are taken into account together with engine indicated efficiency η_i and relative amount of heat transferred to walls by cooling K_{cool} . Pressure losses in all connecting pipes, intercoolers and exhaust gas aftertreatment devices are respected.

The pressure difference between inlet p_{im} and exhaust p_{ex} needed for pre-defined scavenging is calculated from averaged reduced flow area $\mu_{scav} A_{red}$ of engine valves during scavenging period (reversely proportional to the engine flow resistance) and required delivery ratio λ_d

$$\dot{m}_{im} = \mu_{scav} A_{red} \frac{p_{im}}{\sqrt{T_{im}}} \sqrt{\frac{2}{r_{im}} \left(1 - \frac{p_{ex}}{p_{im}} \right)} = \lambda_d \frac{p_{im}}{r_{im} T_{im}} V_s \frac{n_E}{60} \quad (1)$$

Power balance of a turbocharger with a low-pressure compressor outlet pressure p_{C2} , used as supercharger inlet pressure, atmospheric pressure p_a and appropriate pressure differences between machines, with constant pressure thermal capacities c_p and appropriate exponents connecting pressure and temperature ratios during isentropic change with exponent e yields

$$\dot{m}_{im} c_{pC} T_a \left[\left(\frac{p_{C2}}{p_a - \Delta p_{C1}} \right)^{e_c} - 1 \right] = \left(\dot{m}_{im} + \dot{m}_f \right) c_{pT} T_{T1} \eta_{TC} \left[1 - \left(\frac{p_a + \Delta p_{T2}}{p_{exh} - \Delta p_{T1}} \right)^{e_r} \right] \quad (2)$$

Finally, energy balance of an engine with fuel mass-flow rate \dot{m}_f and lower calorific value H_u determined at reference temperature T_{ref} , with the share of cooling losses K_{cool} and indicated efficiency η_i yields for exhaust gas temperature

$$-\left(\dot{m}_{im} + \dot{m}_f \right) c_{pT} (T_{T1} - T_{ref}) + \dot{m}_{im} c_{pC} (T_{im} - T_{ref}) + H_u \dot{m}_f (1 - K_{cool}) = H_u \dot{m}_f \eta_i \quad (3)$$

Fuel mass flow rate can be linked to air mass-flow rate by air excess λ , engine charging efficiency $\eta_{scav}\lambda_{ch}$ and stoichiometric air-to-fuel ratio L_r .

Combining those relations, the dependence of achievable turbocharger compressor pressure ratio on inlet manifold pressure p_{im} with iterated ratios of pressure losses (which do not vary too much during iteration) and, as well, iterated temperature in inlet manifold (dependent on intercooler efficiency) can be found from the equation

$$\left(\frac{p_{C2}}{p_a - \Delta p_{C1}} \right)^{e_c} = 1 + \left\{ 1 + \left[\left(1 + \frac{\eta_{scav}\lambda_{ch}}{\lambda_d\lambda L_t} \right) \frac{c_{pT}}{c_{pC}} - 1 \right] \frac{T_{ref}}{T_a} + \frac{H_u}{c_{pC}T_a} \frac{\eta_{scav}\lambda_{ch}}{\lambda_d\lambda L_t} (1 - K_{cool} - \eta_i) \right\} \times \left[1 - \frac{\left(\frac{p_{exh}}{p_a - \Delta p_{T1}} \frac{p_a + \Delta p_{T2}}{p_a - \Delta p_{C1}} \frac{p_a - \Delta p_{C1}}{p_{im}} \right)^{e_T}}{1 - \frac{1}{2r_{im}T_{im}} \left(\lambda_d V_s \frac{n_E}{60\mu_{scav}A_{red}} \right)^2} \right] \quad (4)$$

Especially in the case of poppet valve gear, the limited accelerations during valve motion limit the averaged area during scavenging. The power of a turbocharger turbine, reduced by low exhaust gas temperature, has to be supported by other energy source, mostly a supercharger coupled in series with a turbocharger compressor and covering the pressure difference between p_{C2} and p_{im} . Unlike the pumping loop of a four-stroke engine the work needed for reaching the pressure difference cannot be recuperated back to engine crankshaft but the supercharger power input has to be added to friction losses, changing thus gross brake power to the final net brake power. The described original procedure makes fast assessment of two-stroke brake efficiency possible while the main parameters of engine are changed in rated mode of operation.

The influence of rated air excess and turbocharger efficiency while other parameters were fixed to values found from experiments and simulations of an extremely downsized two-cylinder diesel engine under development is presented in [Figure 1](#) and [Figure 2](#). The net brake power and net brake fuel consumption is calculated after supercharger power input (dependent on scavenging mass flow-rate, supercharger pressure ratio p_{C2}/p_{C1} , supercharger inlet temperature after intercooling the air from a turbocharger compressor and supercharger isentropic efficiency) is subtracted from the engine gross brake power, dependent on assumed indicated efficiency and gross mechanical efficiency.

The former one shows the influence of a boost pressure on a single cylinder power at fixed trapped air excess (denoted as λ_{im} in [Figure 1](#)) and turbocharger overall efficiency for delivery ratio, charging ratio and scavenging efficiency typical for a tested engine with reversed tumble scavenging. In the current case the charging ratio was approx. 70% and scavenging efficiency approx. 60%, ensuring the charging efficiency close to 40% at a reasonable level of delivery ratio. While indicated and gross brake power at engine speed of 1500 rpm are turbocharger efficiency independent, the net brake power and net brake efficiency strongly depend on turbocharger efficiency, since the missing pressure level needed for scavenging has to be covered by an engine driven supercharger. Moreover, the mixture strength (air excess), which is decisive for pollution level, should be compromised. If set too high, it calls for high inlet manifold pressure for reaching rated power, reducing simultaneously the exhaust gas temperature and decreasing the achievable power of turbine, which is reflected by too low supercharger inlet pressure. Then the difference between gross and net engine parameters is increased.

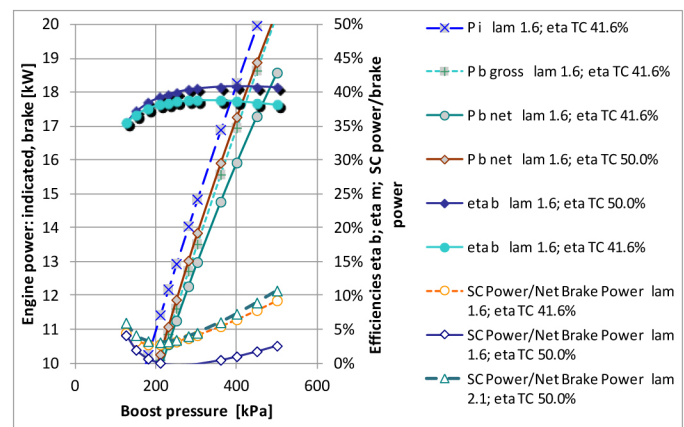


Figure 1. Single cylinder power (indicated, gross brake and net brake - including a supercharger drive), share of supercharger power input on engine net brake power and net brake efficiency in dependence on required boost pressure for different levels of air excess and turbocharger overall efficiency

The share of supercharger power of the engine total shows clearly that there might be no need for a supercharger in some range of power if the efficiency of a turbocharger is high enough and if the excess air is fixed at reasonable mixture strength level (1.6 for the current case). On the other side, the need of high supercharger power input increases if air excess is too high. For this engine operation point the computed exhaust temperature was 480degC.

Those results are confirmed by the [Figure 2](#) in which the pressures close to a supercharger are drawn for two levels of air excess (causing different engine power at the same inlet manifold pressure level, of course). The BSFC is strongly influenced by the air excess chosen and turbocharger efficiency available. The combustion quality and indicated specific fuel consumption was not influenced by air excess too much in this range of mixture richness.

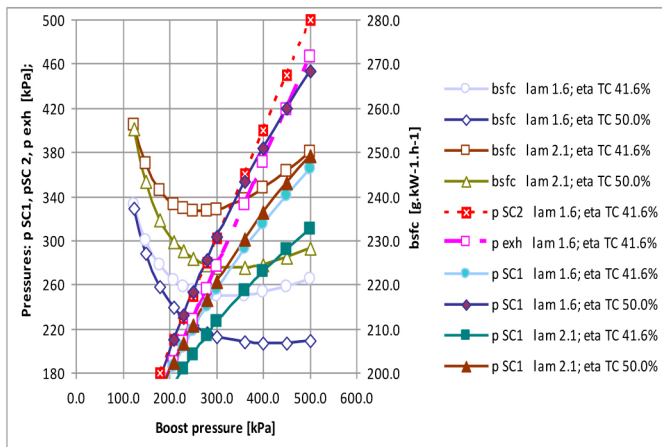


Figure 2. Required averaged pressures at a supercharger and in exhaust manifold and net brake specific fuel consumption in dependence on parameters from the Figure 1

Engine and Working Point Selection

As described in the previous publication [2], the targeted engine platform is based on the Renault K9K 1.5 dCi power unit. The original engine architecture has been adapted to work on a 2 stroke cycle.

The initial objective was to build a GT Power model that would allow performing reliable simulation of multiple air loop design. The purpose of this paper is to summarize the model validation work on engine, the matching optimization and assessment on engine of the new configuration.

The engine main dimensional characteristics are summarized in Table 1.

Table 1. Engine geometrical data

Bore	76	mm
Stroke	80.5	mm
No. of cylinders	2	
Displacement	0.73	l
Connecting rod length	133.8	mm
Compression ratio	17.2	
No. of valves per cyl.	4	

The targeted performances in full load are:

- 45 kW @ 3000 rpm
- 145 Nm from 1000 to 3000 rpm

The simulation was initially performed not only in full load but also in 6 key partial load points, summarized in Table 2. These points are time weighted and representative of the NEDC emission cycle for a Renault Twingo with a mass of 925kg on R14 tires and a drag coefficient of 0.68 equipped with the 2 stroke engine part of this study (see Table 3).

In Figure 3 it can be seen how these operating points, in green, are distributed in the overall homologation cycle, blue "x"s. It was preferred to use time weighted points rather than BSFC weighted points to better represent the effect to the whole cycle duration.

Table 2. Part load points definition

		Point 1	Point 2	Point 3	Point 4	Point 5	Point 6
Engine speed	RPM	1250	1000	1500	2000	1500	2500
Torque	N.m	25	50	50	50	90	130
BMEP	bar	2,15	4,3	4,3	4,3	7,7	11,2
EGR rate	%	20	20	20	20	15	15

Table 3. Part load weighting coefficients

Engine speed [rpm]	1250	1000	1500	2000	1500	2500
Torque [N.m]	25	50	50	50	90	130
Weightening coef. [%]	36.4	17.1	23.2	13.0	7.4	2.9
Equivalent time [s]	385	181	246	138	79	31

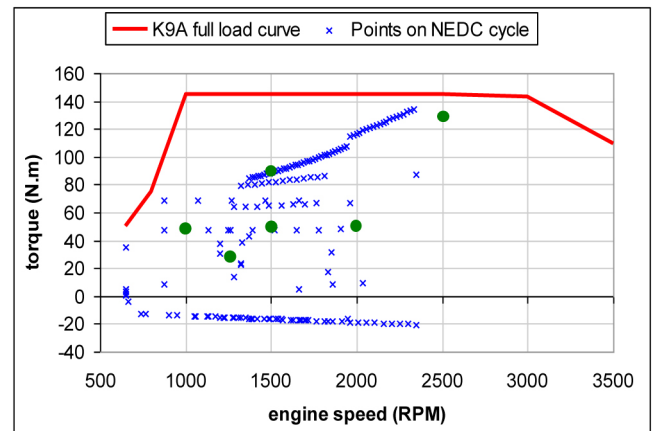


Figure 3. Full load requirements and investigated part load (green) points

Air System Concept Analysis

Initial step for the air system definition has been to analyse similar existing solutions. Two architectures have been identified with the desired characteristics of this study. A 2-stroke engine prototype from AVL (1.0l, 3-cylinder) and a Daihatsu (1.2l, 2-cylinder). Both adopt a serial sequential boosting architecture with a mechanical supercharger and turbocharger. The AVL engine lay out considers the mechanical supercharger arranged downstream of the turbocharger while the Daihatsu adopted a lay out with the mechanical supercharger upstream of the turbocharger [2]. What are the main differences we should expect from those two different solutions? The installation of the mechanical supercharger in the high pressure (HP) stage enables selecting a smaller supercharger than the one required in the low pressure (LP) stage. This facilitates the packaging and reduces the overall engine weight and also allows working at lower supercharger speeds. One drawback we need to consider when working with the supercharger in the HP stage is that it will be working at higher compressor inlet temperatures and this will limit the operating range of the mechanical supercharger and have a higher power demand from the engine crankshaft.

The down selection of the concepts was done keeping all of those aspects in consideration trying to achieve the project performance targets. To facilitate the down selection a concept tree was created as described in [Table 4](#).

Table 4. Overview of the investigated air system concepts

	Low Pressure Stage	High Pressure Stage	EGR loop	TC	Drive system
Mechanical Supercharger	Positive displacement charger - Centrifugal charger	Turbocharger	X Cooled LP or MP	Variable geometry turbine - Fixed geometry turbine	Variable gear ratio - Single gear ratio Dual gear ratio
	Turbocharger	Positive displacement charger - Centrifugal charger			
Electrical Boost devices	Turbocharger	e-Boost			External e-Power
	e-Boost	Turbocharger			
	Turbocharger + TAE (turbine assisted electrically)				

Initial Boosting System Down Selection

The concept tree analysis led to discard the single stage boosting as a viable option due the compression ratio needs and the scavenging characteristic of the 2 stroke engine architecture. Ultimately an initial set of 8 options was identified for the initial assessment in GT Power (see [Table 5](#)).

Table 5. Assessed air system configurations

Type	LP stage	HP stage	Cooled EGR loop
C1	Mechanical positive displacement charger	Turbocharger	LP
C2	Mechanical positive displacement charger	Turbocharger	MP
C3	Turbocharger	Mechanical positive displacement charger	LP and MP
C4	Mechanical centrifugal charger	Turbocharger	LP and MP
C4bis	Turbocharger	Mechanical centrifugal charger	LP and MP
C6	Turbocharger	e-boost	LP and MP
C6bis	e-boost	Turbocharger	LP and MP
C7	Turbocharger	Turbine assisted electrically	LP and MP
C8	Turbine assisted electrically	Turbocharger	LP and MP

All concepts have a two stage boosting layout with a turbocharger either in the low pressure (LP) or high pressure (HP) stage arranged in a “serial sequential” lay out, with mechanically driven positive displacement or centrifugal supercharger with variable, single or dual speed. Further concepts comprise of e-booster and e-turbo.

During the partial load operation it was assessed the possibility to have low pressure (LP) and mid (MP) pressure EGR loops (blended EGR mode).

With reference to the nomenclature in [Table 5](#), in the below [Figure 4](#), the more conventional lay outs are sketched. Supercharger in LP stage C2 (left) and supercharger in HP stage C3 (right) both with middle pressure (MP) EGR loop are presented with following labelling: 1-turbocharger with bypass,

2-LP intercooler, 3-supercharger by-pass, 4-supercharger, 5-supercharger transmission, 6-HP intercooler, 7-engine, 8-EGR loop with EGR valve and intercooler.

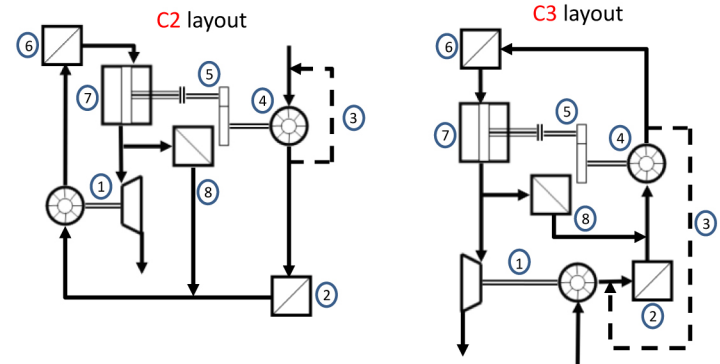


Figure 4. Comparison of LP vs. HP supercharger configuration

The first step for the concept down selection has been to simulate the fuel consumption of the 8 concepts in the NEDC partial load points summarized in [Table 3](#). The results of the most promising options ([Table 6](#)) are plotted in [Figure 5](#), where the x-axis is the time weighted fuel consumption and the z-axis is the technical feasibility index. The feasibility index reflects the parts availability for hardware testing, packaging constrains and performance achievable potential.

Table 6. Best options summary

Configurations	Configurations break down
C2 Pos. displ. charger upstream TC	-a variable drive + VGT
C3 Pos. displ. charger downstream TC	-b dual drive + VGT
C4 Centrifugal charger upstream TC	-c variable drive + turbine WG
C4bis Centrifugal charger downstream TC	-d dual drive + turbine WG

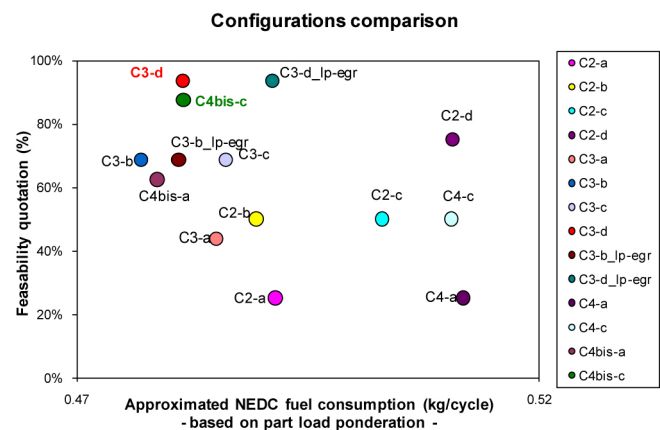


Figure 5. Fuel Consumption comparison of the 8 simulated configurations

The results allow making few general considerations regarding the difference in Fuel Consumption between the HP and LP layout of mechanical supercharger. The supercharger downstream of the turbocharger (HP) enables lower fuel consumption than the LP lay out. LP layout in fact requires the supercharger to spin faster to provide the requested boost as a consequence of the presence of the low pressure loop EGR that increases the compressor inlet temperature. The two speed drive of the supercharger is preferred over the one

speed gear box. On the other hand the variable supercharger drive does not allow any significant fuel benefit in partial load mainly due to the higher mechanical losses.

Based on this consideration and on the data in Figure 5 it has been possible to identify the configuration C3-d, (waste gate fixed geometry turbocharger coupled with positive displacement supercharger downstream and with two speed gearbox, (Figure 6), as the one with highest potential to reach the project objectives in terms of power and fuel consumption reduction. Another interesting option is the C4bis-c with centrifugal charger set downstream of the waste gate turbocharger and the variable supercharger drive (CVT). This one is considered the backup solution by the authors as the hardware is in a less mature stage than the 2 speed supercharger option.

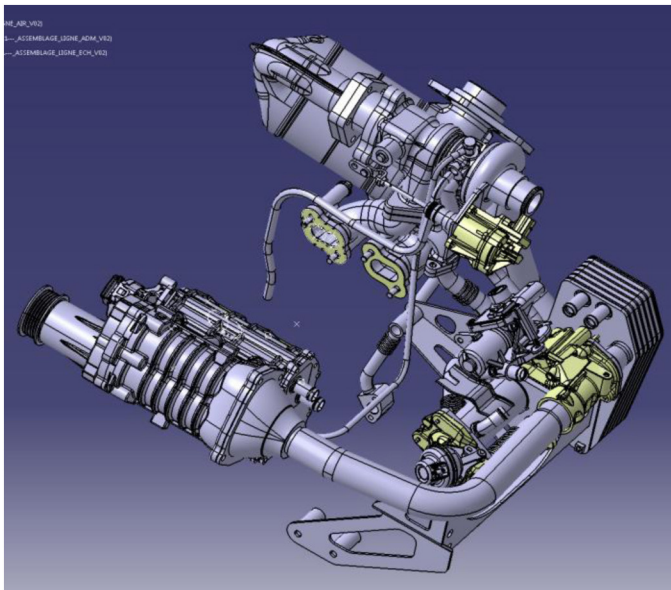


Figure 6. Lay out of the preferred air loop system C3-d. Supercharger downstream of the waste gate turbocharger

Validation of the Simulated Options on Gas Stand

The validation of the turbocharger maps used in the simulation activity was performed in a specialized laboratory using state of the art open loop gas stand measurement methodology. Three units have been tested. The original turbocharger from supplier 1 *TC1* plus 2 more variants *TC2* and *TC3* from an alternative supplier.

Figure 7 compares the compressor efficiencies and flow capacity of the 3 units (all compressors tested at the same circumferential velocity). This highlights that while the compression ratio (PRC) and flow capacity of *TC1* and *TC2* are comparable, *TC3* has the possibility to achieve much higher PRC and efficiency values at low flow rates than the previous two units and hence enables higher low end torque (LET) achievement potential. The surge limits are comparable for all units.

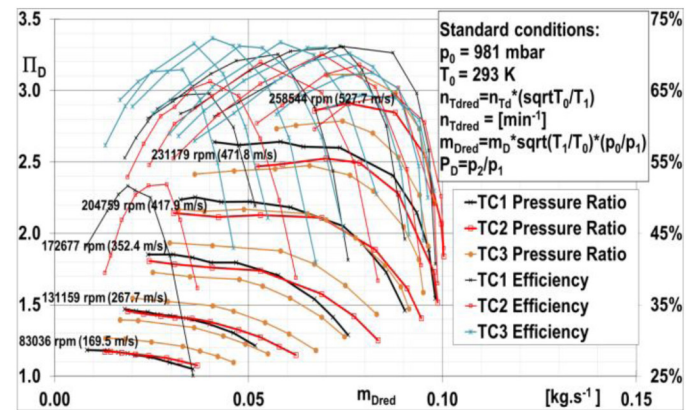


Figure 7. Compressor maps of TC1, TC2, and TC3

Figure 8 shows performance of the original turbine stage (*TC1*) vs. *TC2* and *TC3* options. *TC2* and *TC3* turbine stages improved the efficiency by up to 10pts mainly at expansion ratio higher than 2 vs. the original *TC1*, on the other hand the swallowing capacity was increased by ~10% at expansion ratio of 3. In operating points where the turbine efficiency of the *TC2* & *TC3* is lower than the one achievable by *TC1*, we might experience reduction of the engine low end torque due to the lower turbine power available. Nonetheless, this data clearly show a big performance improvement provided by the new units *TC2* and *TC3* vs. the initial baseline such to recommend reconsidering the matching initially selected.

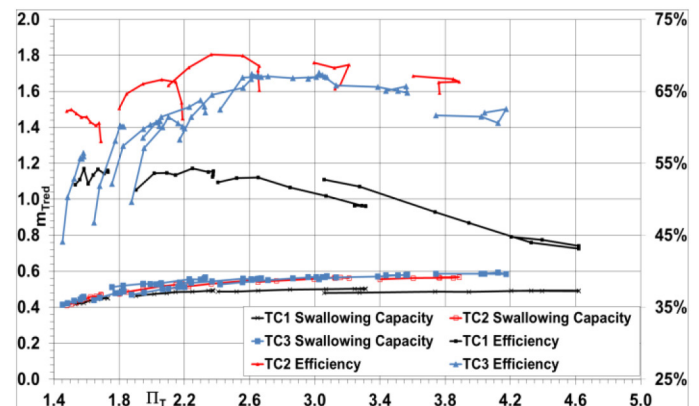


Figure 8. Turbine measurements of TC1, TC2, and TC3

GT Power Model Calibration and Matching Revision

The *TC1* and the selected positive displacement supercharger were tested on the first engine built. The authors used the combustion pressure traces and other key engine input parameters to calibrate the GT-Power model described in Figure 9 and increase the accuracy of the simulation on the subsequent turbo matching optimizations steps.

Main elements that were optimized are:

- Combustion law based on MBV50 data
- More precise scavenging law based on CFD simulation
- Verification of scavenging levels through trace gas (methane) measurement

- Friction losses were extrapolated by measurements on existing engine hardware
- System geometry optimized with engine 3d data

The new matching activity was then performed using the same supercharger selected in the previous paper [2] this time combining it with several Honeywell Turbo Technologies options. The portfolio studied includes fixed geometry waste gate turbocharger configuration as well as variable geometry solutions such as the GTD variable nozzle turbocharger family.

The results are summarized in Table 7 which highlights some interesting differences compared to the results of the non calibrated model. Particularly while the waste gate fixed geometry was not able to meet all the requirements of peak power and low end torque, the GTD variable nozzle turbocharger, not only enabled meeting this objectives, it concurrently allowed to manage more effectively the transition from “super-turbo” mode to turbocharger mode only. Hence the optimal configuration that was identified to be assessed on engine is the GTD1038 with 34mm variable geometry turbine and 38mm compressor.

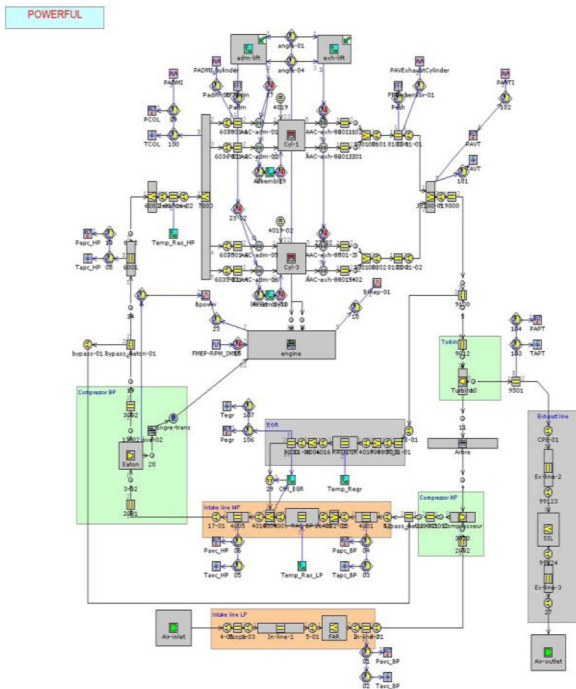


Figure 9. Super turbo configuration in GT Power model

Table 7. Matching summary and main parameter performance

POWERFUL 0.73L diesel 2-stage with T/C in LP and Roots supercharger in HP stage								
T/C framesize	Turbine type	Torque[N.m] @1500 rpm	Peak Power [kW] @3000rpm	P1T [kPa_abs] @3000 rpm	Max. Eaton T2C [degC]	Surge depth (-) or margin (+) [g/s] @1500rpm	Max Turbo speed [krpm]	T/C Speed margin
Unit	-	[N.m]	[kW]	[kPa_abs]	[deg C]	[g/s]	[krpm]	
Target	-	143	45	150	-	-	GT10 290k GT12 270k	10%
0 Baseline Supplier 1	Radial WG	104	45	480	160	25	276	5%
1 GT1038	Radial WG	101	45	420	170	22	254	12%
2 GTD1038	Radial VNT	143	45	365	166	15	257	11%
3 GTD1038	Radial VNT	145	45	376	163	10	256	12%
4 GT1238	Radial WG	125	45	478	178	12	279	overspeeding
4 GT1238	Radial WG	127	45	519	175	20	268	1%

In Figure 10 and Figure 11, can be reviewed the performance of the GTD1038 with the initially selected options. One of the most noticeable advantages is the substantial increase in low end torque, and the reduction of the engine back pressure (P1T). This last factor (P1T), allowed reducing the boost demand to the supercharger, with remarkable advantages in reliability and supercharger outlet temperatures as described in Figure 11.

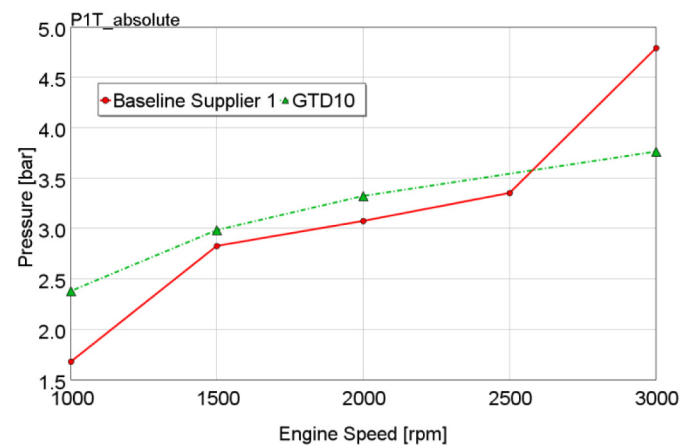
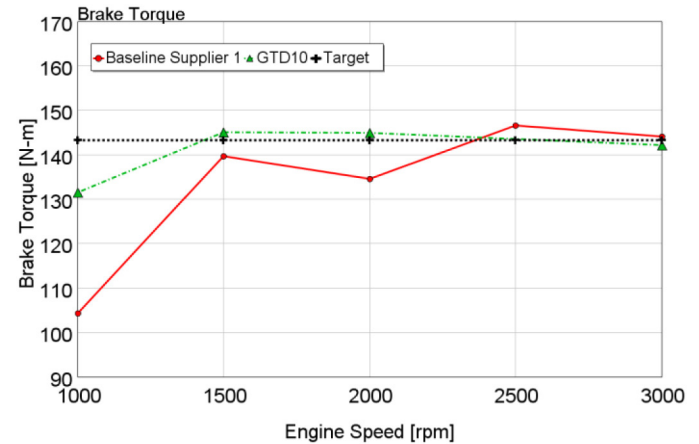


Figure 10. Torque and Engine back pressure improvements

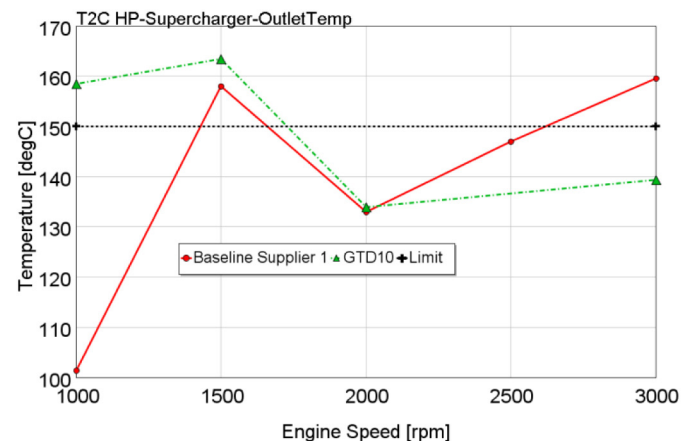


Figure 11. Supercharger outlet temperatures and compression ratio demand

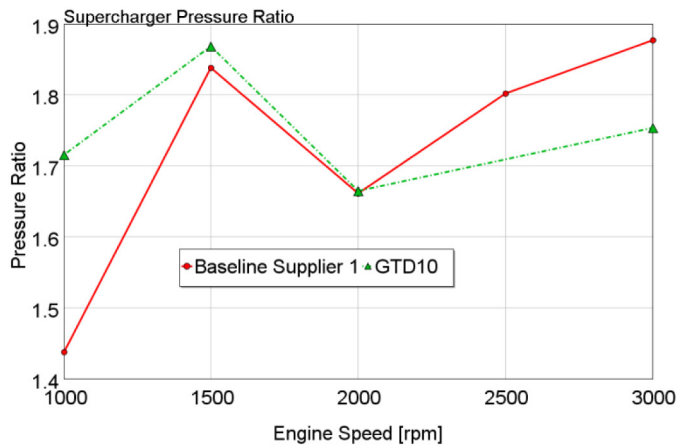


Figure 11. (cont.) Supercharger outlet temperatures and compression ratio demand

Also in Figure 12, it can be seen that the compressor operates in the best efficiency areas in most of its operating points.

In this second round of simulation no partial load tests were simulated for the assessment, as it is planned to perform during the course of 2014 a set of roll bench measurements vehicle tests of the NEDC emission cycle.

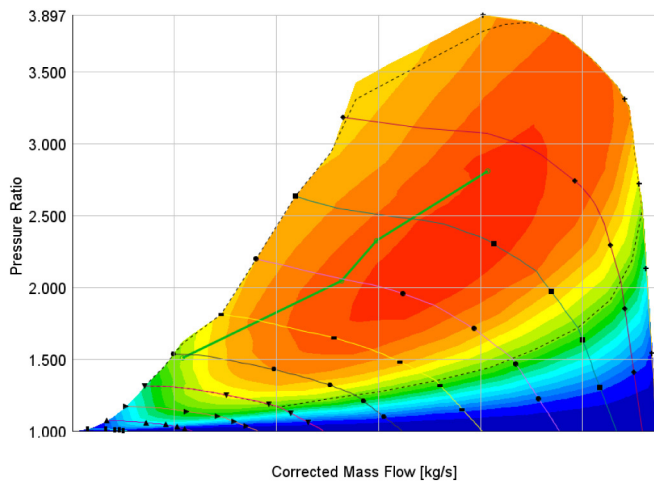


Figure 12. Lug line in the GTD1038 compressor map

Lastly in Figure 13, it can be seen the comparison of BSFC among the 2 new best options. The baseline GTD1038 is capable to provide comparable BSFC but with superior performance (see Figure 10).

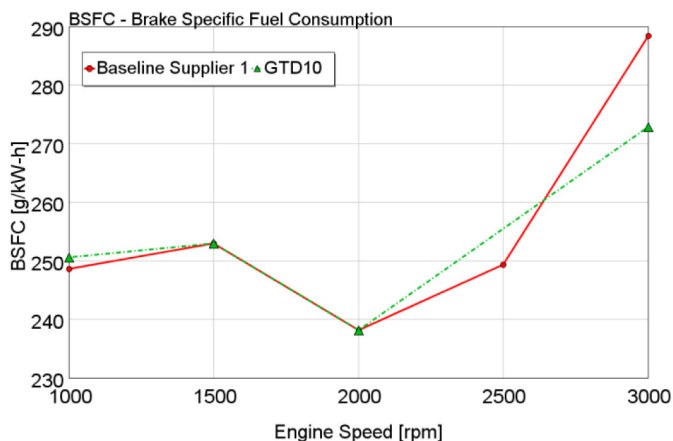


Figure 13. BSFC comparison between baseline and WG and VNT options

Hardware Assessment

Roots - Type Supercharger

Roots supercharger is a positive displacement supercharger with compression ratio depending on pressure in the outlet piping. It uses a shock wave compression to compress the ingested air. Scheme of the used test rig is shown in Figure 14.

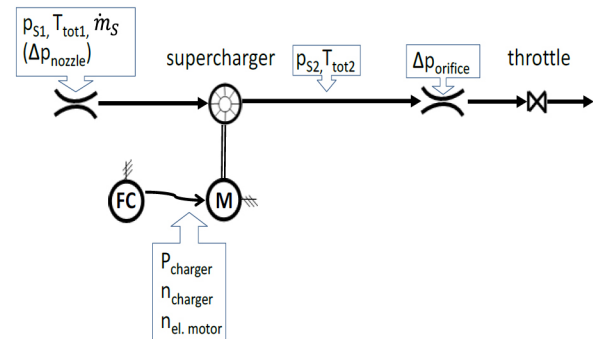


Figure 14. Roots type supercharger test rig scheme

Following Figure 15 presents the supercharger test rig used for supercharger characterization.

The maps prepared with this test results are quite similar to the supercharger performance map used for our simulations as shown in Figure 16 and Figure 17. The isentropic efficiency computed from measured data is even a little bit higher than the one assumed in simulations due to the fact that the compressor map used for GT Power matching included also the compressor internal mechanical efficiency.

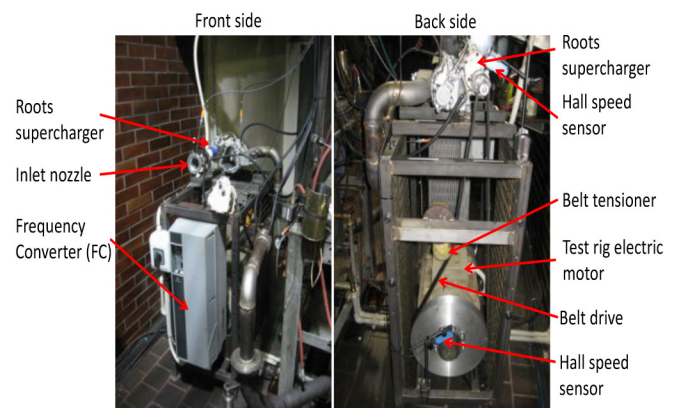


Figure 15. Roots type supercharger test rig

During the Roots type supercharger test campaign the highest pressure ratios at particular speed lines could not be measured due to the outlet air temperature limitation of 170°C (150°C limit assumed for engine simulations). Additionally, the highest speed lines were not verified because of need to modify the step up gear ratio between the test rig electric motor and the supercharger. This gear ratio issue was also identified during the preliminary engine tests. It was then necessary to consider for the test campaign on engine the backup solution with variable drive of centrifugal supercharger as an optimized Roots type supercharger was not available at the time of the engine test campaign start.

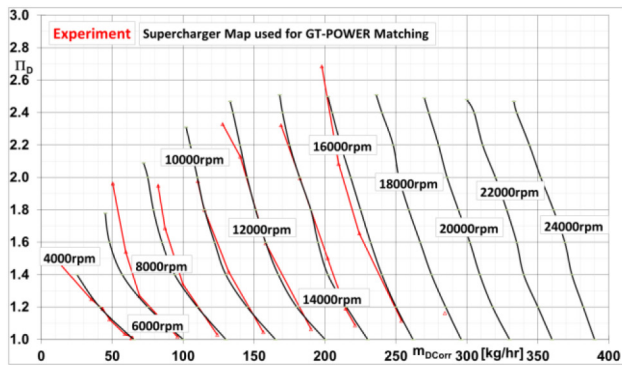


Figure 16. Pressure ratio vs. mass flow rate characteristic of Roots type supercharger

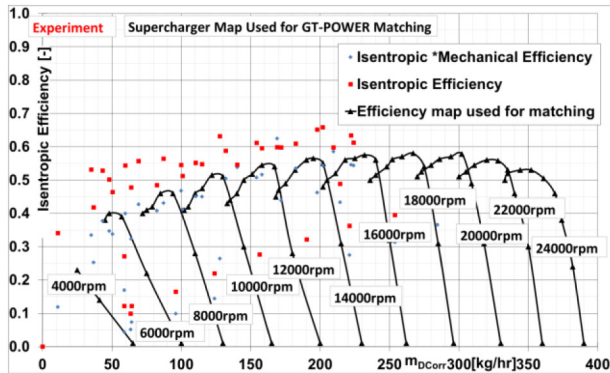


Figure 17. Isentropic efficiency vs. mass flow rate characteristic of Roots type supercharger

Mechanically Driven Centrifugal Supercharger

The test of mechanically driven centrifugal supercharger (back up configuration: C4bis-C + VNT GTD1038) has been done on the same test rig used for the Roots type supercharger and with the same methodology (Figure 14). The centrifugal supercharger had hydraulically controlled transmission ratio of the Continuously Variable Transmission (CVT) instead of the two step speed variation used for Roots supercharger. The control strategy involved one more degree of freedom vs. the Roots supercharger however it has to be noticed that an additional hydraulic pump was needed to operate the unit. The supercharger's CVT measurements are summarized in Table 8. A more detailed look at the device and its size is provided by the Figure 18 and Figure 19. The latter one in particular shows the extra pump needed for the oil circuit.

Table 8. Key operating points and limits of the centrifugal supercharger

Key operating data and limits		
Maximum Variator input speed	[rpm]	21000
Maximum Variator output speed	[rpm]	17500
Maximum Variator ratio	[-]	2.4
Minimum Variator ratio	[-]	0.5
Planetary gearbox step up ratio	[-]	12.51
Maximum Compressor speed	[rpm]	219000
Maximum Variator control pressure	[bar]	25
Minimum Variator control pressure	[bar]	1
Maximum Supercharger oil temperature	[degC]	100
Maximum CVT bearings temperature	[degC]	130

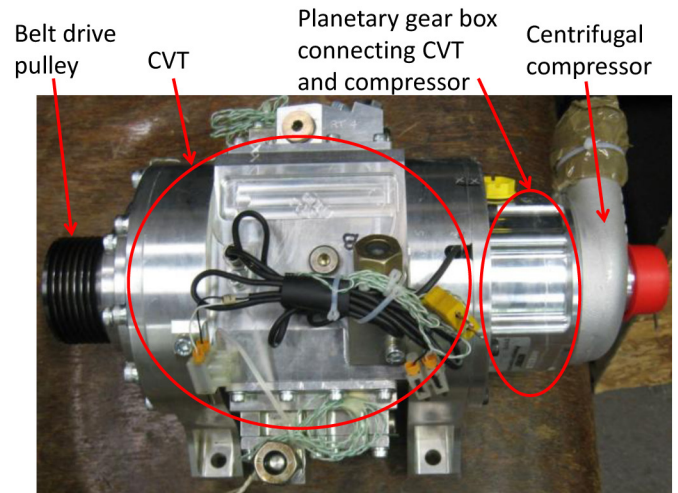


Figure 18. Mechanically driven centrifugal supercharger

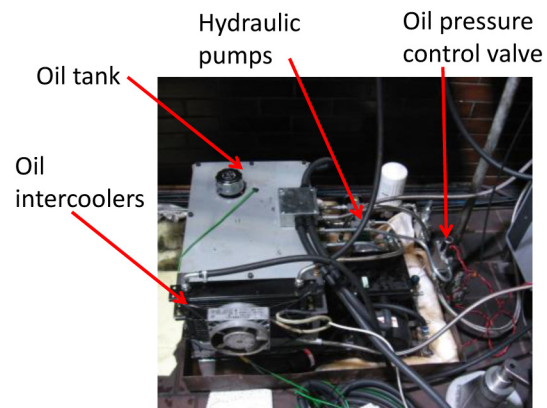


Figure 19. Additional hydraulic equipment

Also in the case of the CVT centrifugal supercharger, the correlation between the map used in the simulation and the measured one is quite good as shown in Figure 20.

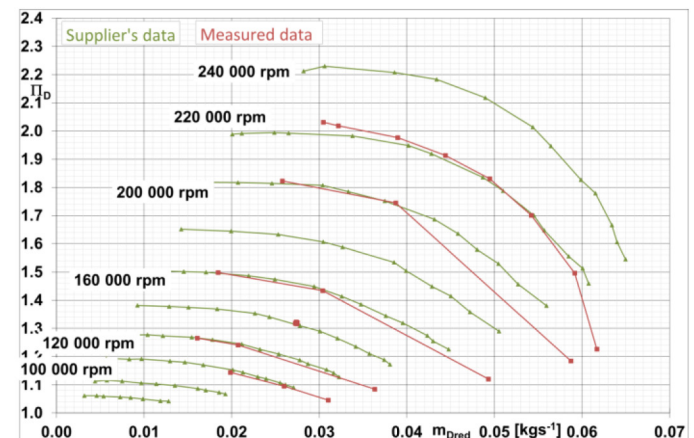


Figure 20. Centrifugal supercharger performance comparison (measured vs. provided for 1-D simulations)

The measured compressor surge appeared to be shifted to the high flow range part of the map vs. the data used in simulation. This might limit the engine performances. Nonetheless, there were not surge issues of the supercharger on the engine.

Concerning the isentropic efficiency there is large difference at low compressor speeds (up to 20%) and small difference (about 2%) at high compressor speed between assumed vs. measured performance as shown in [Figure 21](#).

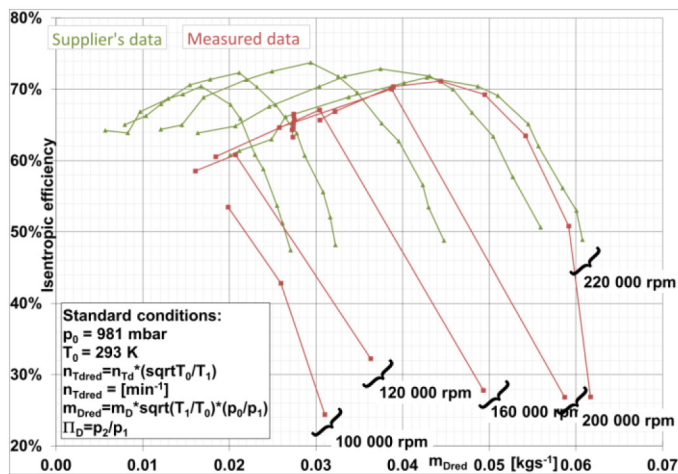


Figure 21. Centrifugal supercharger isentropic efficiency

For the CVT supercharger a full energy balance has been calculated to understand the effective benefit of the system. A rigorous approach to this calculation would require measuring the mechanical efficiency of each subsystem of the device:

$$\eta_{mech_total} = \eta_{belt_drive} \cdot \eta_{CVT} \cdot \eta_{planet_gearbox} \cdot \eta_{compressor} \quad (5)$$

Whereas the elements are:

- The mechanical efficiency of a belt drive connecting test rig electric motor (or combustion engine in a car)
- mechanical efficiency of the CVT;
- mechanical efficiency of planetary gear box connecting CVT and compressor
- Mechanical efficiency of centrifugal compressor.

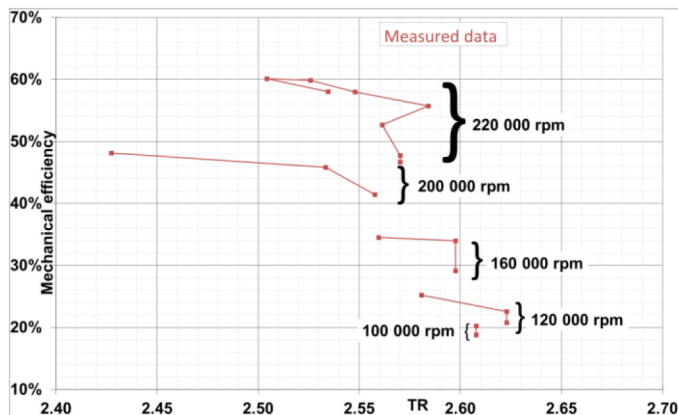


Figure 22. Centrifugal supercharger total mechanical efficiency vs. transmission ratio

Practically, this approach is not achievable without direct measurement of each component individually. It was preferable to obtain the device total mechanical efficiency from the measured electric motor power input and the centrifugal compressor power absorption in each measured operation point. The efficiency results for the measured transmission ratios (TR) are plotted in [Figure 22](#) showing maximum device mechanical efficiency of 60%.

Superchargers Performance Comparison

In [Figure 23](#) there are plotted the performance maps of the two superchargers just described as measured at the steady flow test rig. Based on the main engine speed and load requirements, 5 corresponding supercharger working points have been selected to perform the performance comparison as summarized in [Table 9](#). The comparison, presented in [Table 9](#) and [Figure 24](#), shows approximately double power demand of the variable centrifugal compressor for the same boost requirement. The CVT supercharger is being optimized by the supplier on the basis of current inputs.

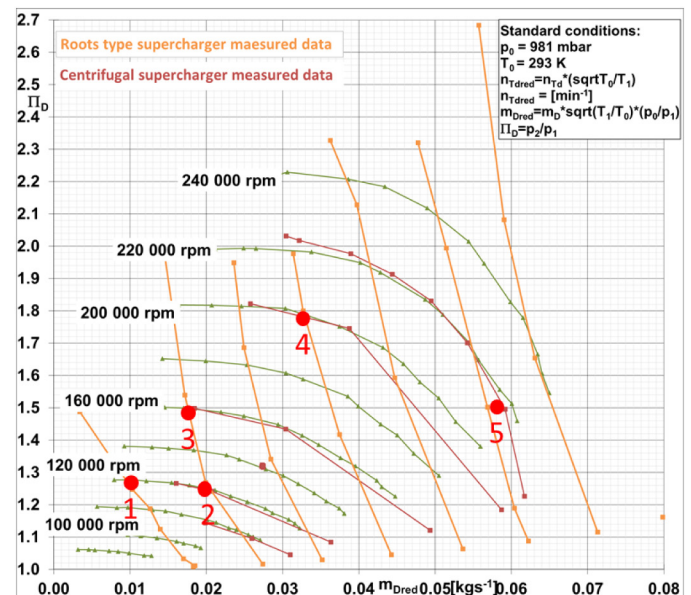


Figure 23. Efficiency of Roots supercharger vs. CVT supercharger

Table 9. Performance comparison points for supercharger assessment

Point Nr.	Mass flow	Pressure ratio	Selected points	
			Test rig electric motor shaft power Roots	Test rig electric motor shaft power Centrifugal
	[kg/s]	[-]	[kW]	[kW]
1	0.010	1.25	0.55	1.97
2	0.020	1.27	0.91	2.90
3	0.017	1.54	1.56	3.34
4	0.033	1.80	3.74	5.63
5	0.057	1.50	3.66	7.23

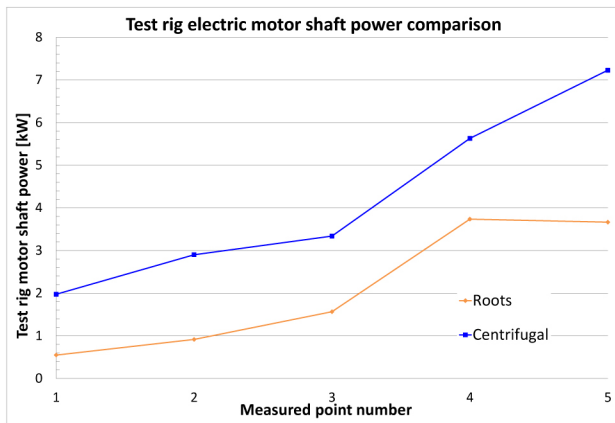


Figure 24. Test rig electric motor power output comparison

On Engine System Assessment

Engine Configuration

The following chapter deals with the tests performed at IFPEN test bench on a multi-cylinder engine. The main objective of the test campaign was to test the air loop configuration, to quantify compatibility, interaction and synergy between turbocharger and supercharger and the 2-strokes engine and power targets achievability.

The investigated configuration is:

- CVT centrifugal supercharger set downstream the turbocharger,
- Honeywell Variable Nozzle Turbocharger,
- Mid pressure EGR loop.

Several temperature and pressure sensors are installed on the engine (see Figure 25). The engine is small, compact and light, 4 valves (no inlet or exhaust ports), to allow compatibility with a four-stroke production line. Figure 26 describes the cam lift profiles.

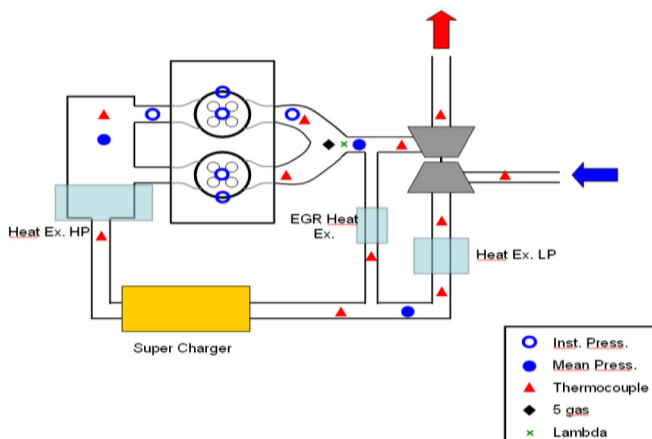


Figure 25. Temp & Pressure Sensor Position

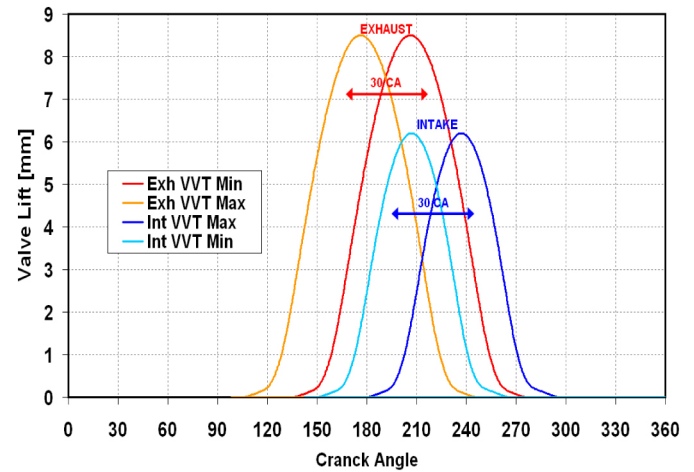


Figure 26. Powerful engine and valve lift set-up

Performance of Honeywell VNT & CVT Centrifugal Supercharger

Two engine speeds have been tested at full load, 1500rpm and 3000rpm. The first step was to optimize the scavenging efficiency of the engine, by controlling the VVT actuators, to get the best trade-off between permeability and in-cylinder air trapping. Moreover, a balance between maximum IMEP and compressor penalty has to be found.

Figure 27 shows the influence of the VVT settings on the air mass flow, FMEP and resulting BMEP. For these tests, the VNT position is constant, and the pressure ratio of the CVT centrifugal supercharger (CVT-SC) is kept constant at 1.7.

Two-stroke engines are very sensitive to the scavenging efficiency, and so to camshaft positions and valve lifts. It is necessary to obtain the best trade-off between high air mass flow (for high IMEP) and low friction due to the supercharger work.

Upon valve lifts optimizing, it is then possible to get the optimal performance of the engine by changing VNT settings. For example, at 1500rpm, the VNT positions have been swept from 20% to 60% (where 100% is the maximum opening).

The tests highlighted that: (1) high opening values, above 60% make the turbine stage work in a range such not to produce enough work on the turbine shaft, and consequently available to the compressor, (2) too low values, below 20% reduce strongly the turbine permeability increasing engine exhaust pressure.

For these tests, the pressure ratio of the CVT-SC is again kept constant at 1.7. The fuel injected quantity is tuned to reach a constant smoke level of 3 FSN, and the start of injection is adapted to have maximal cylinder pressure equal to 140 and 160 bar. For the full load tests, the best performance is obtained with high differential pressure between intake and exhaust manifolds. As described in "Main Issues of Two-Stroke Engine Pressure Charging" chapter, two-stroke engine scavenging efficiency is directly dependant on this differential pressure, even if additional acoustics effects can slightly impact this trade-off.

It is also very important to pay attention and choose the VNT proper parameters in function of the resulting delta P (Figure 28).

The maximal BMEP is obtained when the VNT position is 30%, that is to say when the exhaust pressure is high enough to produce the needed amount of work for the compressor, for a targeted intake pressure up to 4bar. By this way, high value of delta P is obtained, the scavenging is efficient, IGR rate is low and the air mass trapped higher.

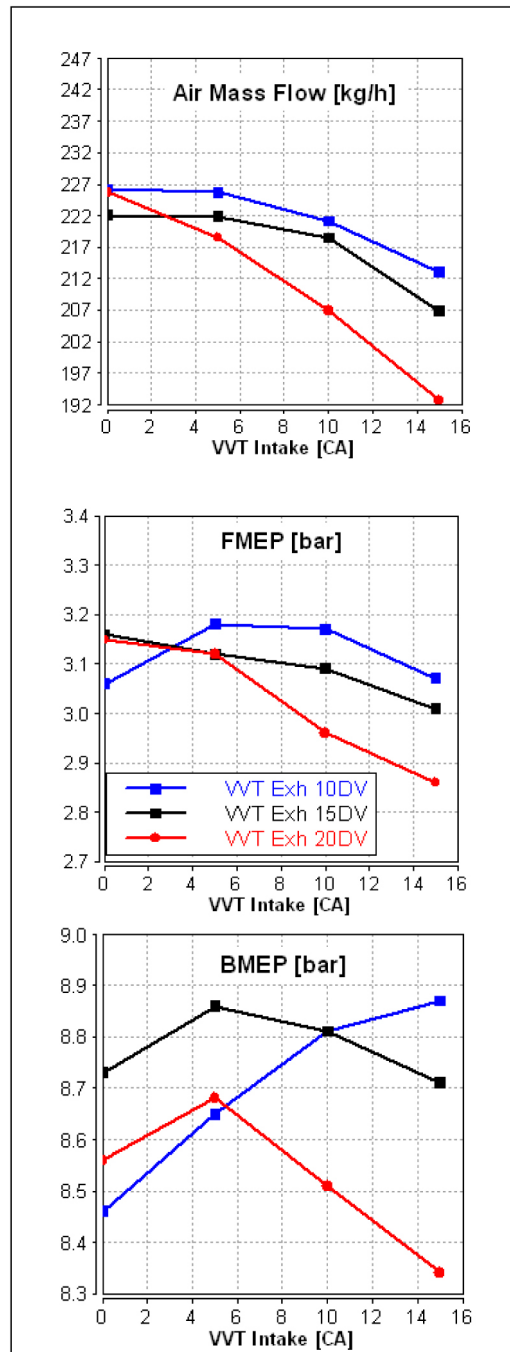


Figure 27. Effects of the VVT settings on the full load performances at 3000rpm

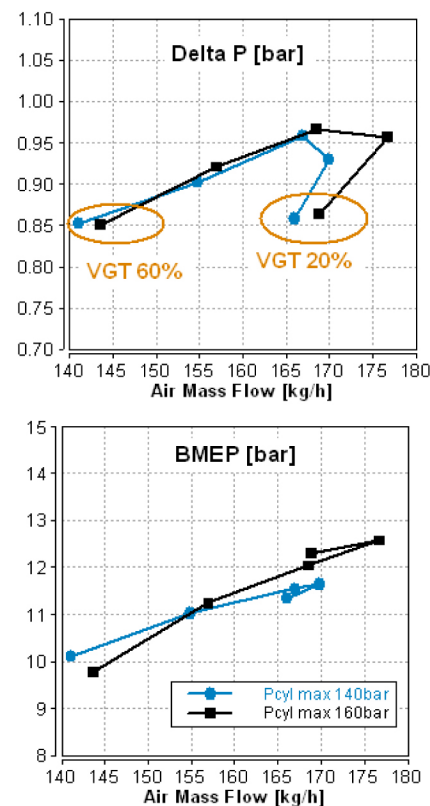


Figure 28. Effect of VNT position on DeltaP and maximal BMEP at 1500rpm

The Honeywell VNT turbine ("VGT") and compressor efficiencies, measured on the engine, are showed in Figure 29. As expected the VNT settings strongly modify the turbine efficiency. The values higher than 61% are promising with respect to waste gate turbines, tested previously in the Powerful project, which had featured higher nominal efficiency but lack of controllability with good efficiency. After WG is opened in the case of high exhaust gas flow-rate, the total efficiency of turbine & WG unused enthalpy head drops down significantly, of course. On the other side, the big efficiency gap of VNT occurs if nozzle is closed too much, namely to turbine efficiency of 57% for the minimum vane opening tested (VGT 20%). Those control ranges should be avoided by a supercharger transmission ratio control. Concerning the compressor, as expected its efficiency increases with air mass flow-rate, to reach value close to 67%.

Finally, it is interesting to plot on the compressor efficiency map the experimental points of the full load test at 1500 and 3000rpm (Figure 30).

Engine Test Conclusion

The full load tests done at IFPEN show that the turbocharger choice, made through 1D simulation, is validated. Indeed, at 1500rpm and 3000rpm, compressor and turbine efficiencies fulfil the original project targets. The fuel consumption data have not been reported as it is planned to have a vehicle test campaign in summer 2014. This should allow having more precise data than the one deduced from the BSFC and the weighting factors.

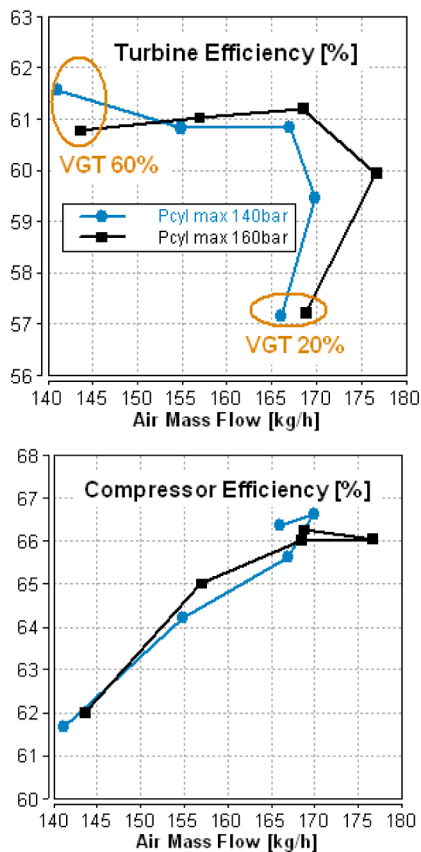


Figure 29. Efficiency of Honeywell turbine and compressor at 1500rpm Full Load

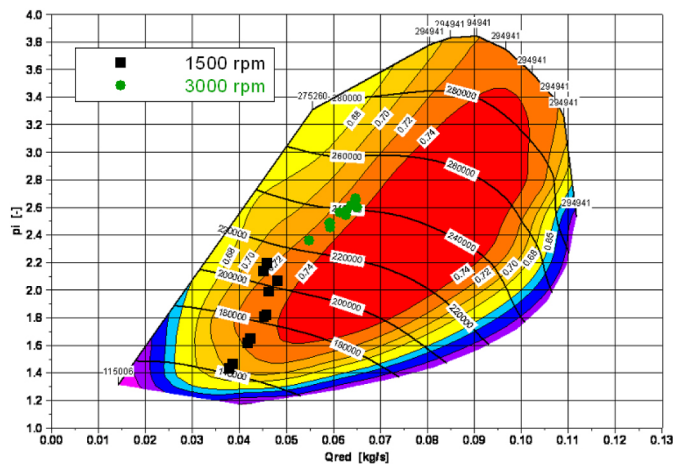


Figure 30. Honeywell compressor efficiency map

Summary/Conclusions

In this paper we have reviewed the results of a GT Power engine model calibration leveraging experimental data from single cylinder combustion test rig, real 2 cylinder engine measurements and turbocharger gas stand performances. The newly calibrated model was used to refine the matching reconsidering the Variable Nozzle Turbine option for the low pressure stage of the boosting system. The simulation results showed that the VNT option is the best solution to deliver the requested performance when coupled either with a Roots supercharger or with the CVT-supercharger.

Additionally an analysis on gas stand of the two possible supercharging solutions has allowed identifying the limits of these machines for this kind of applications. In the case of the Roots supercharger there is the limit in range due to outlet compressor temperatures above certain compression ratios, and in the case of the CVT-supercharger the high power absorption from the engine.

Ultimately a final assessment on fuel consumption and CO₂ reduction potential is now planned for the middle of 2014 given the quite good performances of the powertrain system on the test bench.

References

1. Heywood, J.B., "Internal Combustion Engine Fundamentals," McGraw-Hill, London, England, 1988, ISBN 0-07-028637-X.
2. Pohorelsky, L., Brynych, P., Macek, J., Vallade, P. et al., "Air System Conception for a Downsized Two-Stroke Diesel Engine," SAE Technical Paper [2012-01-0831](#), 2012, doi:[10.4271/2012-01-0831](#).
3. Brynych, P. - Macek, J. - Pohorelský, L., "Air System Proposal and Testing for a Downsized Two-Stroke Diesel Engine," In Proceedings of the FISITA 2012 World Automotive Congress, Beijing, SAE-China, FISITA (Eds.), 2012, Vol. 1, p. 289-314, ISBN 978-3-642-33841-0.
4. Macek, J., Pohorelský, L., "Supercharger and Turbocharger Tests at CZ a.s. Strakonice," ČVUT Praha 2010.
5. Bartelet P., Morand N., Chammas B., Tuissant L., Sausse L., Riviere C., Bouvier E., "The new family of VNT™ turbocharger developed by Honeywell turbo technologies for Euro 6 and beyond," Dresden supercharging conference 2013.
6. GT POWER User's manual and Tutorial GT-Suite™ version 6.2, Gamma Technologies Inc., 2012.
7. Ciesla, C., Keribar, R., and Morel, T., "Engine/Powertrain/ Vehicle Modeling Tool Applicable to All Stages of the Design Process," SAE Technical Paper [2000-01-0934](#), 2000, doi:[10.4271/2000-01-0934](#).
8. Morel, T., Keribar, R., and Leonard, A., "Virtual Engine/ Powertrain/Vehicle" Simulation Tool Solves Complex Interacting System Issues," SAE Technical Paper [2003-01-0372](#), 2003, doi:[10.4271/2003-01-0372](#).

Acknowledgments

This research has been sponsored by the European Union in framework of the POWERFUL project, seventh framework program FP7/2007-2013, theme 7, sustainable surface transport, grant agreement No. SCP8-GA-2009-234032. The co-sponsoring of this EU project was covered by the Ministry of Education, Czech Republic, as project #7E10051.

The part of the research has been supported by the project Josef Bozek Competence Centre for Automotive Industry #TE 01020020, granted by the Technological Agency of Czech republic.

Finally, the support of EU Regional Development Fund in OP R&D for Innovations (OP VaVpl) and Ministry for Education, Czech Republic, project # CZ.1.05/2.1.00/03.0125 Acquisition of Technology for Vehicle Center of Sustainable Mobility has been used. These supports are gratefully acknowledged.

Further, the authors would like to thank Ludek Pohorelsky and Paolo Di Martino for their support during the research work and compilation of herewith presented work.

Definitions/Abbreviations

1 - inlet

2 - outlet

C - compressor

CVT - continuously variable transmission

DPF - diesel particulate filter

EGR - exhaust gas recirculation

FC - frequency convertor

IGR - internal gas recirculation

M - electric motor

MBV50 - mean burn value

PCCI - premixed charge compression ignition

T - turbine

VGT - variable geometry turbocharger

VNT - variable nozzle turbocharger

VVT - variable valve train

BMEP [bar] - break mean effective pressure

BSFC [g/kW/h] - break specific fuel consumption

c_p [J/kg/K] - thermal capacity

e [-] - exponents of isentropic change

FMEP [bar] - friction mean effective pressure

FSN [-] - filter smoke number

H_u [MJ/kg] - lower calorific value

IMEP [bar] - indicated mean effective pressure

K_{cool} [-] - cooling loss coefficient

L_f [-] - stoichiometric air-to-fuel ratio

\dot{m}_f [kg/s] - fuel mass-flow rate

\dot{m}_{im} [kg/s] - inlet port mass flow rate

n_E [rpm] - engine speed

p_a [kPa] - atmospheric pressure

p_{C2} [kPa] - compressor outlet pressure

p_{ex} [kPa] - engine exhaust pressure

p_{im} [kPa] - inlet manifold pressure

T_{im} [K] - inlet manifold temperature

T_{ref} [K] - reference temperature

V_s [m³] - engine displacement volume

λ [-] - trapped air excess

λ_{ch} [-] - charging ratio

λ_d [-] - delivery ratio

$\mu_{scav} A_{red}$ [m²] - averaged engine reduced flow area

η_b [-] - engine brake efficiency

η_i [-] - engine indicated efficiency

η_m [-] - engine mechanical efficiency

η_{sc} [-] - total supercharger efficiency

η_{scav} [-] - scavenging efficiency

η_{TC} [-] - total turbocharger efficiency

The Engineering Meetings Board has approved this paper for publication. It has successfully completed SAE's peer review process under the supervision of the session organizer. The process requires a minimum of three (3) reviews by industry experts.

All rights reserved. No part of this publication may be reproduced, stored in a retrieval system, or transmitted, in any form or by any means, electronic, mechanical, photocopying, recording, or otherwise, without the prior written permission of SAE International.

Positions and opinions advanced in this paper are those of the author(s) and not necessarily those of SAE International. The author is solely responsible for the content of the paper.

ISSN 0148-7191

<http://papers.sae.org/2014-32-0011>